JOURNAL OF APPLIED PHYSICS VOLUME 96, NUMBER 7 1 OCTOBER 2004

Electrical transport in $ZnO_{1-\delta}$ films: Transition from band-gap insulator to Anderson localized insulator

Ashutosh Tiwari,[a] C. Jin, and J. Narayan
NSF Center of Advanced Materials and Smart Structures, Department of Materials Science & Engineering, North Carolina State University, Raleigh, North Carolina 27695-7916

M. Park
Department of Physics, Auburn University, Auburn, Alabama 36849

(Received 9 January 2004; accepted 22 June 2004; publisher error corrected 9 February 2005)

We have thoroughly investigated the effect of oxygen nonstoichiometry on the electrical transport characteristics of $ZnO_{1-\delta}$ films. These films were grown on optical grade quartz substrates by using a pulsed laser deposition technique. In order to alter the amount of oxygen nonstoichiometry (δ), oxygen partial pressure during the film growth was systematically varied from 10^2 Torr to 10^{-5} Torr. Qualitative estimates about the amount of oxygen nonstoichiometry in these films were made using Raman Spectroscopy data. High resolution electrical resistivity and thermoelectric power measurements were performed in the temperature range 12–300 K. A detailed analysis of electrical transport data showed a transition from band-gap insulating state (for the films prepared at high oxygen environments) to Anderson localized insulating state (for the films prepared at lower oxygen environments). © *2004 American Institute of Physics*. [DOI: 10.1063/1.1783591]

INTRODUCTION

During the past few years, zinc oxide thin films have attracted considerable scientific and technological attention.[1–5] It is a direct band gap material with a band gap of 3.3 eV and exciton binding energy of 60 meV. Because of its higher exciton binding energy, it is considered a promising substitute of GaN in various short-wavelength optical and light emitting applications. Moreover, ZnO exhibits quite a high n-type electrical conductivity[6,7] which can further be increased by doping or by creating oxygen vacancies in the material for transparent conductor applications.

A lot of theoretical as well as experimental work has undergone to understand the electrical transport mechanism in ZnO, but still the picture is not very clear and more precise understanding of the electrical transport properties of this material is desired. In this paper we have made an effort to understand the electrical transport in $ZnO_{1-\delta}$ films, prepared under varying oxygen pressure. Variation of oxygen partial pressure presumably results in systematic changes in oxygen vacancy concentration which are expected to cause interesting changes in the electrical transport mechanism. For our investigations, we have used temperature dependent (12–300 K) thermoelectric power and electrical resistivity measurement techniques.

Thermoelectric power S is an important tool for studying the nature of charge carriers and various processes that occur close to the Fermi surface.[8,9] It is defined as the voltage developed across the two ends of the sample when a unit temperature gradient is applied between them. Thermoelectric power of metals varies linearly with temperature ($S \sim T$) while for insulators and semiconductors it follows a hyperbolic temperature dependence and is given by the expression[8]

$$S = \frac{K_B}{e}\left(\frac{E_C - E_F}{K_B T}\right), \tag{1}$$

where K_B is the Boltzmann constant, and E_C and E_F are the positions of the lower edge of conduction and Fermi level, respectively.

The value of S for semiconductor materials depends upon the amount of dopant (or oxygen vacancies), the energy levels of the dopant states, the energy gap, and the temperature. These factors determine the number of carriers per unit volume and, thus, are major factors influencing the electrical conductivity also. However, the above expression is valid only for the band-gap insulators, where, the Fermi level lies in the forbidden gap between the conduction band and the valence band. In the case of Anderson localized insulators,[10] where the density of states is finite at E_F (though these states are localized), the expression for thermoelectric power is

$$S = \frac{1}{2}\frac{K_B}{e}\frac{W^2}{K_B T}\left(\frac{d \ln N(E)}{dE}\right)_{E=E_F}, \tag{2}$$

where $W = K_B(T_0 T^3)^{1/4}$; K_B is the Boltzmann constant, $N(E)$ is the density of states, and T_0 is a constant. According to this expression in the case of Anderson localized insulators, S varies as $\sqrt{T}$ and approaches to zero as $T \rightarrow 0$ K.

EXPERIMENT

For the present investigations, $ZnO_{1-\delta}$ films were prepared by a pulsed laser deposition technique, where oxygen partial pressure was varied systematically from 100 Torr to 10^{-5} Torr (see Table I). Depositions were performed on optical grade quartz substrates at 650 °C inside a stainless steel chamber. Thickness of all the films was kept same at 200 nm. Films were characterized using x-ray diffraction (Cu-$K\alpha$ radiation), transmission electron micros-

---

[a] Electronic mail: atiwari@unity.ncsu.edu

0021-8979/2004/96(7)/3827/4/$22.00

TABLE I. Room temperature thermoelectric power S(300 K) and electrical resistivity ρ(300 K) of $ZnO_{1-\delta}$ films prepared under varying oxygen environment.

Sample number	O_2 Pressure (Torr)	S (300 K)	ρ (300 K) (mΩ cm)
1	100	5.2 mV/K	242.9
2	10^{-1}	−95 μV/K	167.3
3	10^{-3}	−55 μV/K	116.5
4	10^{-5}	−37 μV/K	31.8

copy, and Raman spectroscopy. Electrical conductivity and thermoelectric power measurements on these films were performed with a closed cycle refrigerator in the temperature range 12–300 K. For thermoelectric power measurements dc differential technique with copper as the other arm of the thermocouple was employed. A temperature difference ΔT of 1–2 K was applied across the two ends of the sample and the voltage differential ΔV developed across the sample was measured using a Keithely nanovoltmeter (model 182). The ratio $\Delta V/\Delta T$ gives the thermoelectric power of the sample with respect to copper. The absolute thermoelectric power was obtained by adding to this quantity the absolute thermoelectric power of copper, which was obtained from the literature.[8] Electrical resistivity measurements were performed by standard four-point-probe technique.

RESULTS AND DISCUSSION

Figure 1 shows the x-ray diffraction (XRD) pattern of the ZnO film prepared at 100 Torr of oxygen pressure (sample 1). In the 2θ range 20°–100° we observed only two peaks, which correspond to (0002) and (0004) planes of ZnO. This indicates *c* axis preferred orientation of the film. Films prepared at lower oxygen pressure showed similar XRD pattern except for a slight increase in the *c* axis lattice parameter due to reduced oxygen stoichiometry.

One of the most important factors that affect electrical transport in oxides is its oxygen stoichiometry itself. So, for any careful electrical transport study of oxides, the first and most important step is to determine oxygen stoichiometry. But, exact quantitative determination of oxygen stoichiometry in thin films is an extremely difficult task. However, a qualitative estimate can be made using several indirect techniques like Raman spectroscopy, x-ray photoemission spectroscopy (XPS), Rutherford backscattering, etc. Among those Raman spectroscopy[11] is the most preferable technique for getting relative estimates of oxygen vacancy concentration in thin films via the determination of vacancy induced strain. Oxygen vacancies in $ZnO_{1-\delta}$ cause tensile strain in the film, which results in a shift in the position of Raman peaks. By doing a systematic analysis of Raman data, a qualitative estimate of relative concentration of oxygen vacancies in the films can be made.

ZnO has wurtzite structure which belongs to the $C_{6v}^{4}(P6_3mc)$ space group. According to group theory, following optical modes are allowed at the Γ point of the Brillouin zone of the ZnO:[12]

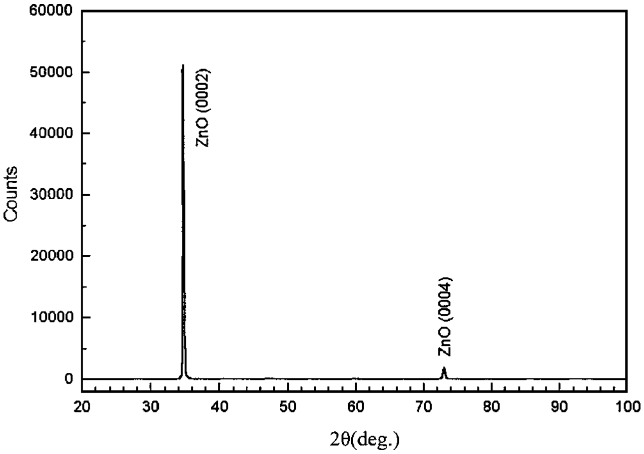

FIG. 1. X-ray diffraction data of ZnO film prepared at 100 Torr of oxygen pressure.

$$\Gamma = \mathbf{A}_1(\mathbf{TO},\mathbf{LO}) + 2\mathbf{B}_1 + \mathbf{E}_1(\mathbf{TO},\mathbf{LO}) + 2\mathbf{E}_2$$

Among these optical modes, $\mathbf{B}_1$ modes are silent, while, $\mathbf{A}_1$, $\mathbf{E}_1$, and $\mathbf{E}_2$ modes are Raman active. The $\mathbf{A}_1$ and $\mathbf{E}_1$ modes are polarized along and perpendicular to the *c* axis of ZnO, respectively. The $\mathbf{E}_2$ mode has two submodes, designated as $\mathbf{E}_2^{(1)}$ (low frequency submode) and $\mathbf{E}_2^{(2)}$ (high frequency submode). The $\mathbf{E}_2^{(2)}$ mode is very sensitive to any kind of strain in the film. It has been widely reported that the presence of tensile strain in films causes a decrease in the frequency shift of $\mathbf{E}_2^{(2)}$ submode.[12,13]

In Fig. 2 we have shown the $\mathbf{E}_2^{(2)}$ Raman peaks for various $ZnO_{1-\delta}$ films. As can clearly be seen from this figure, the position of $\mathbf{E}_2^{(2)}$ peak shifts systematically towards the lower frequency side for the films prepared in lower oxygen pressure (see inset). This suggests the increasing amount of tensile strain and hence higher concentration of oxygen vacancies in the films prepared at lower oxygen ambient. At this point we find it appropriate to mention that the strain in thin films can arise because of two other factors also, namely (i) lattice mismatch and (ii) thermal mismatch between the substrate and the film. However, since all of our films were

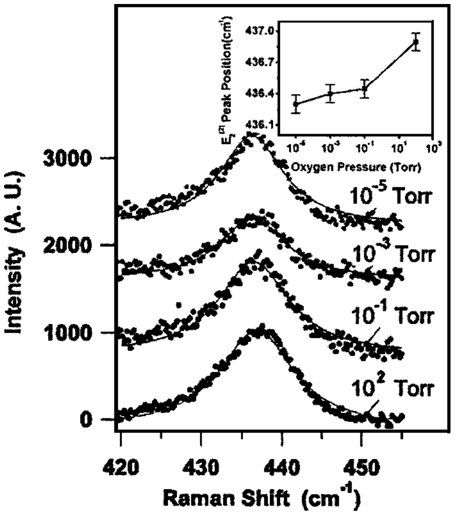

FIG. 2. Raman spectra for various $ZnO_{1-\delta}$ films. Inset shows the variation in the position of $E_2^{(2)}$ peak with oxygen pressure during the thin film growth.

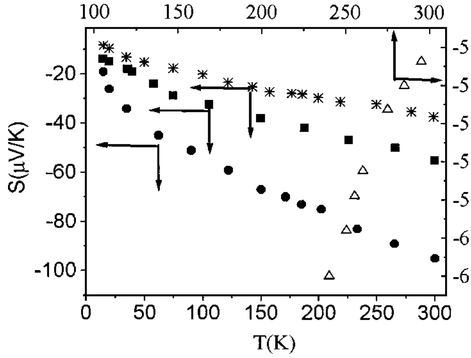

FIG. 3. Thermoelectric power data for various $ZnO_{1-\delta}$ Films. For film 1 vertical scale is shown on the right while for all other films it is on the left. Horizontal scale on the top corresponds to film 1. Symbols △, ●, ■, and * represent films 1, 2, 3, and 4, respectively.

deposited on the amorphous substrate (quartz) under the identical conditions (apart from the oxygen pressure), we believe that the observed systematic change in the tensile strain in these films is mainly because of the change in the concentration of oxygen vacancies.

Thermoelectric power data for various $ZnO_{1-\delta}$ samples are shown in Fig. 3. Some salient features of this data are (a) thermoelectric power of all the samples is negative indicating electrons as the dominant charge carriers,[8,9] (b) magnitude of the thermoelectric power decreases with increasing oxygen deficiency, (c) for the film 1 (prepared under the partial oxygen pressures of 100 Torr) magniture of S increases with decrease in temperature while for all other films (prepared under lower oxygen pressures) the magnitude of S decreases with the decrease in the temperature. In Table I we have tabulated the room temperature thermoelectric power of all the samples. Room temperature thermoelectric power of ZnO prepared at 100 Torr of oxygen is 5.2 mV/K, characteristic of a typical high band-gap semiconductor, while for other films the magnitude of S is about two orders of magnitude smaller. In Fig. 4 we have fitted the thermoelectric power data for film 1 to Eq. (1). From this, we found that Fermi level lies about 1.5 eV below the conduction band. This value is in good agreement with the band gap of 3.3 eV for intrinsic ZnO, a slight shift of Fermi level towards the conduction band indicates that even in the ZnO film prepared at 100 Torr of oxygen pressure some donor states are present. Smaller values of the thermoelectric power for the films prepared under oxygen deficient conditions indicate higher carrier concentration in these films. However, the most striking feature of this data is that the dS/dT exhibits different signs for the films prepared at high and low oxygen environments. For the films prepared at 100 Torr of oxygen pressure dS/dT is positive, while for the films prepared at lower oxygen environments dS/dT is negative. As discussed earlier, the smaller values of S with negative dS/dT indicate that the material has turned either to metallic state or to an Anderson localized insulating state. In order to find the real state of the sample, i.e., whether the samples are metallic or Anderson localized insulators we fitted our experimental data to linear ($S \propto T$) and square root ($S \propto \sqrt{T}$) temperature dependent expressions. In Fig. 5 we have shown the fits and in Table II we have tabulated the values of χ^2 (quality of fit). As can clearly be seen, thermoelectric power data fit better with $\sqrt{T}$ type of temperature dependence implying the Anderson localized insulating state of the films. At this point we want to mention that in the above analysis we have assumed that the observed thermoelectric power of ZnO is only because of the diffusion component. However, in certain cases, phonon drag component may also be important.[8] So in order to authenticate the predictions of thermoelectric power experiment it is essential to verify those using other experimental tools.

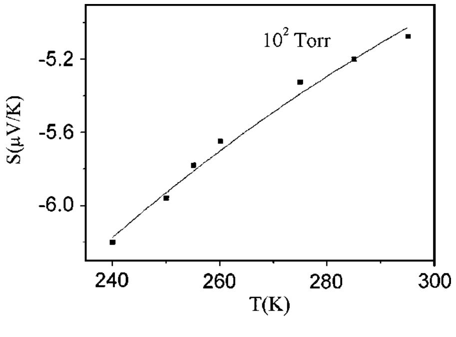

FIG. 4. Least squares fits of thermoelectric power data of film 1 to Eq. (1).

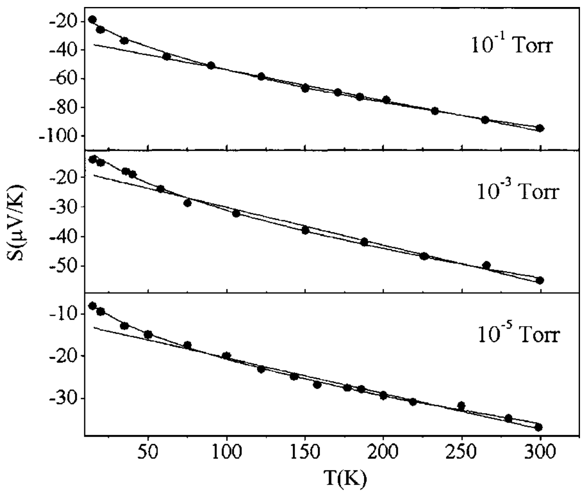

FIG. 5. Least squares fits of thermoelectric power data of films 2, 3, and 4 to linear ($S \propto T$) and square root ($S \propto \sqrt{T}$) temperature dependent expressions.

Temperature dependent electrical resistivity measurement is another very powerful method to distinguish metals from the insulators and band-gap insulators from the Anderson localized insulators.[8,10] Metals exhibit positive temperature coefficient of resistivity (TCR), while insulators show

TABLE II. χ^2 values for the fit of thermoelectric power to $S \propto T$ and $S \propto \sqrt{T}$, and electrical resistivity data to $\ln \rho \propto 1/T$ and $\ln \rho \propto 1/T^{1/4}$. Smaller values of χ^2 for $S \propto \sqrt{T}$ and $\ln \rho \propto 1/T^{1/4}$ imply the Anderson localized insulating state of the films.

	χ^2		χ^2	
Sample number	$S \propto T$	$S \propto \sqrt{T}$	$\ln \rho \propto 1/T$	$\ln \rho \propto 1/T^{1/4}$
2	8.1×10^{-2}	1.8×10^{-3}	1.2×10^{-3}	1.3×10^{-5}
3	2.7×10^{-2}	2.6×10^{-3}	6.7×10^{-3}	8.4×10^{-6}
4	1.7×10^{-2}	5.7×10^{-4}	9.6×10^{-2}	7.0×10^{-6}

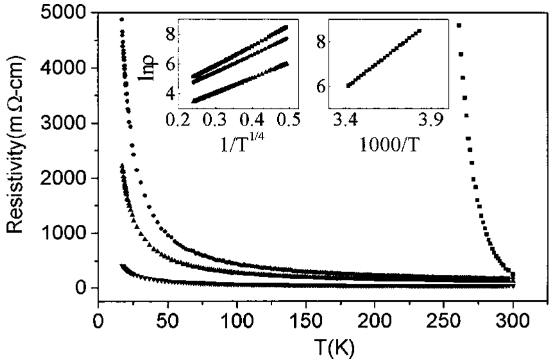

FIG. 6. Electrical resistivity data for various $ZnO_{1-\delta}$ films. Right inset shows the $\ln\rho$ vs $1/T$ plot for film 1. Left inset shows the $\ln\rho$ vs $1/T^{1/4}$ plots for films 2, 3, and 4.

negative TCR. Furthermore, in the case of band-gap insulators,[8] electrical resistivity follows the expression $\ln\rho \propto 1/T$, while for Anderson localized insulators[10] it follows the expression $\ln\rho \propto (1/T)^{1/4}$.

In Table I we have tabulated room temperature electrical resistivity of these films. Room temperature electrical resistivity of the films decreases with the decrease in the oxgen pressure implying higher carrier concentration in oxygen deficient films. Figure 6 shows the temperature dependent electrical resistivity data for various films. For film 1 the electrical resistivity of the film was so high that we could not perform measurements below 260 K using our experimental setup. For other films the measurements were performed down to 12 K. As can be seen from this figure, these films exhibit negative temperature coefficient of resistivity, confirming the insulating nature of the films. We found that for film 1 electrical resistivity fits well in $\ln\rho \propto 1/T$, while for all other films it follows $\ln\rho \propto (1/T)^{1/4}$ (see insets in Fig. 6 and Table II). These results, once again, imply the transition from band-gap insulating state (for film 1) to Anderson localized insulating state (for all other films) in excellent agreement with thermoelectric power data.

Now in order to understand the observed phase transition from band-gap insulating state to Anderson localized insulating state, it is essential to investigate the variation of the electronic levels with doping concentration (i.e., oxygen nonstoichiometry). For intrinsic semiconductors, Fermi level lies very close to the center of the band gap. When the donors are introduced in the semiconductors, discrete energy levels are formed at an energy E_d below the conduction band. Because of donor states, the Fermi level of the doped material shifts from its intrinsic position towards the conduction band. Due to this shift, the value of E_C-E_F decreases, and hence the magnitude of thermoelectric power is expected to decrease. But when donor concentration is very high and hence these centers are closely spaced, they tend to interact with each other and then the system can no longer be described in terms of the discrete impurity levels below the conduction band. Instead, an impurity band appears close to the conduction band. As the concentration of donor further increases, impurity band gets broadened and comes still closer to the conduction band, and under the degenerate conditions it starts to overlap with the conduction band resulting in a nonzero value of density of states at the Fermi level. Under these conditions material may exhibit metallic behavior. This kind of *M-I* transition has been observed in several doped semiconductors in the degenerate limit.[14] However, if the disorder in the system is large enough, the electronic states can become localized resulting in an Anderson localized insulating state.[10,14] We believe that above phenomenon is responsible for the observed electrical transport behavior of $ZnO_{1-\delta}$ system. Random distribution of oxygen vacancies in the material may be responsible for the disorder in the system which results in the localization of electronic states.

CONCLUSION

In conclusion, in this paper we have investigated electrical transport mechanism in $ZnO_{1-\delta}$ films. A transition from band-gap insulating state to Anderson localized insulating state has been observed with increasing oxygen nonstoichiometry. Electrical transport in oxygen deficient Anderson localized $ZnO_{1-\delta}$ films is dominated by the variable-range hopping conduction of charge carriers between the localized states.

ACKNOWLEDGMENTS

The authors want to thank Dr. R. J. Nemanich for permission to use his micro-Raman spectrometer. One of the authors (A.T.) wants to thank Surabhi Pandey for her help in preparing the manuscript.

[1] H. Ohno, Science **281**, 951 (1998).
[2] Z. K. Tang, G. K. L. Wong, P. Yu, M. Kawasaki, A. Ohtomo, H. Koinuma, and Y. Segawa, Appl. Phys. Lett. **72**, 3270 (1998).
[3] D. M. Bagall, Y. F. Chen, Z. Zhu, T. Yao, S. Koyama, M. Y. Shen, and T. Goto, Appl. Phys. Lett. **70**, 2230 (1997).
[4] J. K. Furdyna, J. Appl. Phys. **64**, R29 (1988).
[5] A. Tiwari, C. Jin, A. Kvit, D. Kumar, J. F. Muth, and J. Narayan, Solid State Commun. **103**, 459 (2002).
[6] S. B. Zhang, S. H. Wei, and A. Zunger, Phys. Rev. B **63**, 075205 (2001).
[7] E.-C. Lee, Y.-S. Kim, Y.-G. Jin, and K. J. Chang, Phys. Rev. B **64**, 085120 (2001).
[8] J. S. Dugdale, *The Electrical Properties of Metals and Alloys* (Adward Arnold, London, 1977).
[9] D. D. Pollock, *Thermoelectricity: Theory, Thermometry, Tool* (ASTM, Philadelphia, 1985).
[10] N. F. Mott, *Conduction in Non-Crystalline Materials* (Clarendon Press, Oxford, 1993), Vol. 2.
[11] G. A. Kourouklis, A. Jayaraman, B. Batlogg, R. J. Cava, M. Stavola, D. M. Krol, E. A. Rietman, and L. F. Schneemeyer, Phys. Rev. B **36**, 8320, 1987.
[12] A. Tiwari, M. Park, C. Jin, H. Wang, D. Kumar, and J. Narayan, J. Mater. Res. **17**, 2480 (2002).
[13] S. S. Mitra, O. Brafman, W. B. Daniels, and R. K. Crawford, Phys. Rev. B **186**, 942 (1969).
[14] R. F. Milligan, T. F. Rosenbaum, R. N. Bhatt, and G. A. Thomas, in *Electron-electron Interactions in Disordered Systems*, edited by A. L. Efros and M. Pollak (North-Holland, Netherlands,).